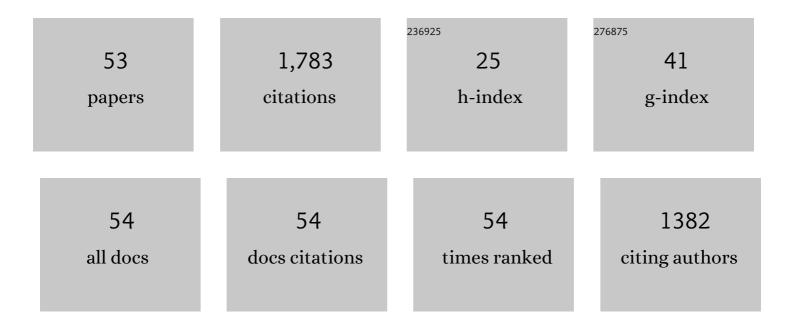
Kalin Kouzmanov

List of Publications by Year in descending order

Source: https://exaly.com/author-pdf/5902455/publications.pdf Version: 2024-02-01



#	Article	IF	CITATIONS
1	Geology, mineralogy, and cassiterite geochronology of the Ayawilca Zn-Pb-Ag-In-Sn-Cu deposit, Pasco, Peru. Mineralium Deposita, 2022, 57, 481-507.	4.1	12
2	Behavior of critical metals in metamorphosed Pb-Zn ore deposits: example from the Pyrenean Axial Zone. Mineralium Deposita, 2021, 56, 685-705.	4.1	35
3	Multistage development of a hydrothermal W deposit during the Variscan late-orogenic evolution: the Puy-les-Vignes breccia pipe (Massif Central, France). Bulletin - Societie Geologique De France, 2021, 192, 33.	2.2	10
4	Osmium isotopic constraints on sulphide formation in the epithermal environment of magmatic-hydrothermal mineral deposits. Chemical Geology, 2021, 564, 120053.	3.3	11
5	Fluid mixing as primary trigger for cassiterite deposition: Evidence from in situ δ18O-δ11B analysis of tourmaline from the world-class San Rafael tin (-copper) deposit, Peru. Earth and Planetary Science Letters, 2021, 563, 116889.	4.4	23
6	Co-Ni-arsenide mineralisation in the Bou Azzer district (Anti-Atlas, Morocco): Genetic model and tectonic implications. Ore Geology Reviews, 2021, 134, 104128.	2.7	9
7	Tracking fluid mixing in epithermal deposits – Insights from in-situ δ18O and trace element composition of hydrothermal quartz from the giant Cerro de Pasco polymetallic deposit, Peru. Chemical Geology, 2021, 576, 120277.	3.3	8
8	Distribution of indium, germanium, gallium and other minor and trace elements in polymetallic ores from a porphyry system: The Morococha district, Peru. Ore Geology Reviews, 2021, 136, 104236.	2.7	16
9	T-P-fO2 conditions of sulfide saturation in magmatic enclaves and their host lavas. Lithos, 2021, 398-399, 106313.	1.4	2
10	Metasomatism and cyclic skarn growth along lithological contacts: Physical and geochemical evidence from a distal Pb Zn skarn. Lithos, 2021, 400-401, 106408.	1.4	5
11	The upper Oligocene San Rafael intrusive complex (Eastern Cordillera, southeast Peru), host of the largest-known high-grade tin deposit. Lithos, 2021, 400-401, 106409.	1.4	6
12	Multiple rejuvenation episodes of a silicic magma reservoir at the origin of the large diatreme-dome complex and porphyry-type mineralization events at Cerro de Pasco (Peru). Lithos, 2020, 376-377, 105766.	1.4	10
13	Tourmaline as a Tracer of Late-Magmatic to Hydrothermal Fluid Evolution: The World-Class San Rafael Tin (-Copper) Deposit, Peru. Economic Geology, 2020, 115, 1665-1697.	3.8	43
14	Alluvial record of an early Eocene hyperthermal within the Castissent Formation, the Pyrenees, Spain. Climate of the Past, 2020, 16, 227-243.	3.4	7
15	Pathways for 39Ar loss during step-heating of alkali feldspar megacrysts from the Shap granite (UK): Combined evidence from diffusion experiments and characterisation of heating-induced texture modifications. Chemical Geology, 2020, 547, 119677.	3.3	4
16	Porphyry and epithermal deposits in Greece: An overview, new discoveries, and mineralogical constraints on their genesis. Ore Geology Reviews, 2019, 107, 654-691.	2.7	38
17	Multiple fluids involved in granite-related W-Sn deposits from the world-class Jiangxi province (China). Chemical Geology, 2019, 508, 92-115.	3.3	62
18	Experimental evidence for mineral-controlled release of radiogenic Nd, Hf and Pb isotopes from granitic rocks during progressive chemical weathering. Chemical Geology, 2019, 507, 64-84.	3.3	28

KALIN KOUZMANOV

#	Article	IF	CITATIONS
19	Mineralized breccia clasts: a window into hidden porphyry-type mineralization underlying the epithermal polymetallic deposit of Cerro de Pasco (Peru). Mineralium Deposita, 2018, 53, 919-946.	4.1	26
20	Cyclic Dilution of Magmatic Metal-Rich Hypersaline Fluids by Magmatic Low-Salinity Fluid: A Major Process Generating the Giant Epithermal Polymetallic Deposit of Cerro de Pasco, Peru. Economic Geology, 2018, 113, 825-856.	3.8	38
21	Fluid Inclusion Studies in Opaque Ore Minerals: I. Trace Element Content and Physical Properties of Ore Minerals Controlling Textural Features in Transmitted Near-Infrared Light Microscopy. Economic Geology, 2018, 113, 1845-1860.	3.8	11
22	Fluid Inclusion Studies in Opaque Ore Minerals: II. A Comparative Study of Syngenetic Synthetic Fluid Inclusions Hosted in Quartz and Opaque Minerals. Economic Geology, 2018, 113, 1861-1883.	3.8	15
23	Incremental Growth of Mid- to Upper-Crustal Magma Bodies During Arabia–Eurasia Convergence and Collision: A Petrological Study of the Calc-Alkaline to Shoshonitic Meghri–Ordubad Pluton (Southern Armenia and Nakhitchevan, Lesser Caucasus). Journal of Petrology, 2018, 59, 931-966.	2.8	21
24	Nature and evolution of fluids associated with specularite-bearing Fe and Au-PGE (Jacutinga) mineralization during the Brasiliano orogeny in the eastern São Francisco Craton, Minas Gerais, Brazil. Ore Geology Reviews, 2017, 86, 130-153.	2.7	13
25	Sulfide Minerals in Hydrothermal Deposits. Elements, 2017, 13, 97-103.	0.5	97
26	Trace element diffusion and incorporation in quartz during heating experiments. Contributions To Mineralogy and Petrology, 2017, 172, 1.	3.1	31
27	Evidence for Residual Melt Extraction in the Takidani Pluton, Central Japan. Journal of Petrology, 2017, 58, 763-788.	2.8	59
28	Enargite-luzonite hydrothermal vents in Manus Back-Arc Basin: submarine analogues of high-sulfidation epithermal mineralization. Chemical Geology, 2016, 438, 36-57.	3.3	21
29	Oxygen isotope heterogeneity of arc magma recorded in plagioclase from the 2010 Merapi eruption (Central Java, Indonesia). Geochimica Et Cosmochimica Acta, 2016, 190, 13-34.	3.9	20
30	Heterogeneous melt and hypersaline liquid inclusions in shallow porphyry type mineralization as markers of the magmatic-hydrothermal transition (Cerro de Pasco district, Peru). Chemical Geology, 2016, 447, 93-116.	3.3	38
31	Sulfide Replacement Processes Revealed by Textural and LA-ICP-MS Trace Element Analyses: Example from the Early Mineralization Stages at Cerro de Pasco, Peru. Economic Geology, 2016, 111, 1347-1367.	3.8	47
32	A refined genetic model for the Laisvall and Vassbo Mississippi Valley-type sandstone-hosted deposits, Sweden: constraints from paragenetic studies, organic geochemistry, and S, C, N, and Sr isotope data. Mineralium Deposita, 2016, 51, 639-664.	4.1	23
33	Timing of porphyry (Cu-Mo) and base metal (Zn-Pb-Ag-Cu) mineralisation in a magmatic-hydrothermal system—Morococha district, Peru. Mineralium Deposita, 2015, 50, 895-922.	4.1	32
34	A Middle Ordovician Age for the Laisvall Sandstone-Hosted Pb-Zn Deposit, Sweden: A Response to Early Caledonian Orogenic Activity. Economic Geology, 2015, 110, 1779-1801.	3.8	18
35	Zoned Base Metal Mineralization in a Porphyry System: Origin and Evolution of Mineralizing Fluids in the Morococha District, Peru. Economic Geology, 2015, 110, 39-71.	3.8	93
36	Tennantite-tetrahedrite series from the Madan Pb-Zn deposits, Central Rhodopes, Bulgaria. Mineralogy and Petrology, 2014, 108, 515-531.	1.1	22

#	Article	IF	CITATIONS
37	Gold speciation and transport in geological fluids: insights from experiments and physical-chemical modelling. Geological Society Special Publication, 2014, 402, 9-70.	1.3	146
38	COPPER-EXCESS STANNOIDITE AND TENNANTITE-TETRAHEDRITE AS PROXIES FOR HYDROTHERMAL FLUID EVOLUTION IN A ZONED CORDILLERAN BASE METAL DISTRICT, MOROCOCHA, CENTRAL PERU. Canadian Mineralogist, 2012, 50, 719-743.	1.0	37
39	Why large porphyry Cu deposits like high Sr/Y magmas?. Scientific Reports, 2012, 2, 685.	3.3	147
40	TEXTURE AND COMPOSITION OF Pb-BEARING PYRITE FROM THE COKA MARIN POLYMETALLIC DEPOSIT, SERBIA, CONTROLLED BY NANOSCALE INCLUSIONS. Canadian Mineralogist, 2012, 50, 1-20.	1.0	29
41	Hydrothermal Controls on Metal Distribution in Porphyry Cu (-Mo-Au) Systems. , 2012, , .		47
42	Fluid evolution in zoned Cordilleran polymetallic veins — Insights from microthermometry and LA-ICP-MS of fluid inclusions. Chemical Geology, 2011, 281, 293-304.	3.3	55
43	Direct Analysis of Ore-Precipitating Fluids: Combined IR Microscopy and LA-ICP-MS Study of Fluid Inclusions in Opaque Ore Minerals. Economic Geology, 2010, 105, 351-373.	3.8	81
44	Late Cretaceous porphyry Cu and epithermal Cu–Au association in the Southern Panagyurishte District, Bulgaria: the paired Vlaykov Vruh and Elshitsa deposits. Mineralium Deposita, 2009, 44, 611-646.	4.1	36
45	Micro-crystalline inclusions analysis by PIXE and RBS. Nuclear Instruments & Methods in Physics Research B, 2008, 266, 2375-2378.	1.4	2
46	Magmatic Fluids in the Breccia-Hosted Epithermal Au-Ag Deposit of Rosia Montana, Romania. Economic Geology, 2006, 101, 923-954.	3.8	63
47	1: Subduction, slab detachment and mineralization: The Neogene in the Apuseni Mountains and Carpathians. Ore Geology Reviews, 2005, 27, 13-44.	2.7	64
48	1-2: Epithermal Pb–Zn–Cu(–Au) deposits in the Baia Mare district, Eastern Carpathians, Romania. Ore Geology Reviews, 2005, 27, 48-49.	2.7	6
49	1-1: Porphyry Cu–Au and epithermal Au–Ag deposits in the southern Apuseni Mountains, Romania. Ore Geology Reviews, 2005, 27, 46-47.	2.7	10
50	MANGANILVAITE, CaFe2+Fe3+(Mn, Fe2+)(Si2O7)O(OH), A NEW MINERAL OF THE ILVAITE GROUP FROM Pb Zn SKARN DEPOSITS IN THE RHODOPE MOUNTAINS, BULGARIA. Canadian Mineralogist, 2005, 43, 1027-1042.	1.0	14
51	Fluid inclusions in sphalerite as negative crystals: a case study. European Journal of Mineralogy, 2002, 14, 607-620.	1.3	13
52	INFRARED MICROTHERMOMETRY AND CHEMISTRY OF WOLFRAMITE FROM THE BAIA SPRIE EPITHERMAL DEPOSIT, ROMANIA. Economic Geology, 2002, 97, 415-423.	3.8	38
53	Morphology, origin and infrared microthermometry of fluid inclusions in pyrite from the Radka epithermal copper deposit, Srednogorie zone, Bulgaria. Mineralium Deposita, 2002, 37, 599-613.	4.1	41